Supporting Information

SBA-15 Supported Fe, Ni, Fe-Ni Bimetallic Catalysts for Wet Oxidation of Bisphenol-A

Suranjana V. Mayani, Vishal J. Mayani, and Sang Wook Kim*

*Department of Advanced Materials Chemistry, College of Science and Technology, Dongguk University, Gyeongbuk 780-714, Korea. *E-mail: swkim@dongguk.ac.kr*
Received July 23, 2014, Accepted August 18, 2014

Synthesis of Fe/SBA-15

SBA-15 was synthesized by a hydrothermal crystallization method as described previously.[1-3] Briefly, 4.0 g P123 was dispersed in 30 g of distilled water and stirred for 3 h, to the resulting solution 120 g of 2 N HCl was added under stirring and finally 9.5 mL of TEOS was added drop wise as silica source. The mixture was continuously stirred at 313 K for 24 h, then transferred into a teflon-lined autoclave and aged for 48 h at 313 K. The product was filtered, washed and dried at 383 K in air. The obtained sample was calcined at 823 K in air for 6 h; Yield: 6.3 g. **Fe/SBA-15** sample was prepared by wet impregnation using $Fe(NO_3)_3{\cdot}9H_2O$ as iron precursor. Equal amount of $Fe(NO_3)_3{\cdot}9H_2O$ (1 g) and SBA-15 (1 g) were dissolved in minimum volume of deionized water (10 mL) under stirring condition for 60 min. The mixture was dried at 353 K, calcined in air at 823 K for 3 h, and obtained **Fe/SBA-15**; Yield: 1.9 g. The dried material was ground well and sieved using 400 mesh (0.037 mm) size test sieves. FTIR (KBr) ν: 457, 695, 790, 960, 1079, 1229, 1380, 1446, 1635, 1638, 2340, 3436 cm^{-1}. ICP analysis of **Fe/SBA-15** catalyst showed 11.8 wt % iron metal.

Synthesis of Ni/SBA-15

Ni/SBA-15 sample was prepared by using $Ni(NO_3)_2{\cdot}6H_2O$ as nickel precursor. In wet impregnation method, equal amount of $Ni(NO_3)_2{\cdot}6H_2O$ (1 g) and SBA-15 (1 g) were mixed in minimum volume of deionized water (10 mL) under stirring condition for 1 h. The mixture was dried at 353 K, calcined in air at 823 K for 3 h and **Ni/SBA-15** was obtained; Yield: 1.9 g. The dried material was ground well and sieved using 400 mesh (0.037 mm) size test sieves. FTIR (KBr) ν: 803, 1369, 1425, 1461, 1637, 1699, 3464 cm^{-1}. ICP analysis of **Ni/SBA-15** catalyst showed 15.3 wt % nickel metal.

Synthesis of Fe-Ni/SBA-15

Fe-Ni/SBA-15 sample was prepared by using $Fe(NO_3)_3{\cdot}9H_2O$ as iron and $Ni(NO_3)_2{\cdot}6H_2O$ as nickel precursors. In wet impregnation method, $Fe(NO_3)_3{\cdot}9H_2O$ (1g), $Ni(NO_3)_2{\cdot}6H_2O$ (1 g) and of SBA-15 (2 g) were mixed in 30 mL of deionized water under stirring condition for 1 h. The mixture was dried at 353 K, calcined in air at 823 K for 3 h and **Fe-Ni/SBA-15** was obtained; Yield: 3.9 g. The dried material was ground well and sieved using 400 mesh (0.037 mm) size test sieves. FTIR (KBr) ν: 484, 799, 987, 1085, 1836, 2030, 3448 cm^{-1}. ICP analysis of **Fe-Ni/SBA-15** catalyst showed 4.9 wt % iron and 7.2 wt % nickel metal.

Catalytic Wet Oxidation of Bisphenol A

Catalytic oxidation was carried out in a batch reactor equipped with a condenser under atmospheric pressure. After the reaction was over, mixture was centrifuged and the reactants remaining unconverted were estimated by spectrophotometer (Varian, Cary-4000, USA). Calibration curves obtained with a minimum of 5 standards were used for quantification of the results. The total conversion of bisphenol A was computed from the decrease in concentration of bisphenol A. The percentage conversion is calculated according to the relation:

$$\text{Conversion (\%)} = [(C_0 - C_t)/C_0] \times 100 \quad (1)$$

Where C_0 is the initial concentration (mol L^{-1}), C_t the concentration at any time after the reaction starts, t the time (min). Gas chromatography-mass spectrometry (GC-MS, Shimadzu GC 2010, USA) was used for product identification.

Physico-chemical Characterization

Powder X-ray Diffractions (PXRD) Analysis. The powder X-ray diffraction was used to characterize the crystalline structure of the catalysts. PXRD patterns of SBA-15 showed characteristic low angle peaks at $2\theta = 0.95^o$, 1.59^o, 1.83^o. The hexagonal lattice with the major peak assigned to the reflection from the (100) plane and two minor peaks with lower intensity corresponding to reflections from the (110) and (200) planes[1,2,4] were observed. Upon functionalization of SBA-15 with inorganic metals (Fe, Ni and Fe-Ni bimetallic), the intensity of all the peaks decreased marginally with a small shift in the 2θ values. XRD peaks were observed at $2\theta = 1.03^o$, 1.45^o, 1.81^o (**Fe/SBA-15**), 0.93^o, 1.55^o, 1.77^o (**Ni/SBA-15**) and 0.93^o, 1.59^o, 1.87^o (**Fe-Ni/SBA-15**), respectively (Figure 1Q, R, S). This might be due to the presence of metal inside the pores, which causes an increase in the scattering power within the pores, resulting in an overall loss

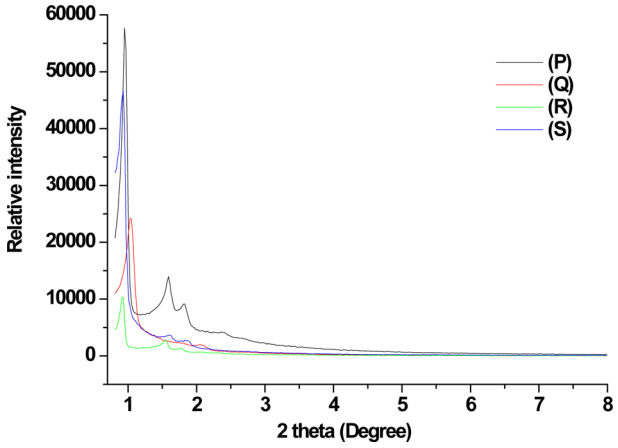

Figure 1. Low angle Powder XRD of SBA-15(P), **Fe/SBA-15**(Q), **Ni/SBA-15**(R) and **Fe-Ni/SBA-15**(S).

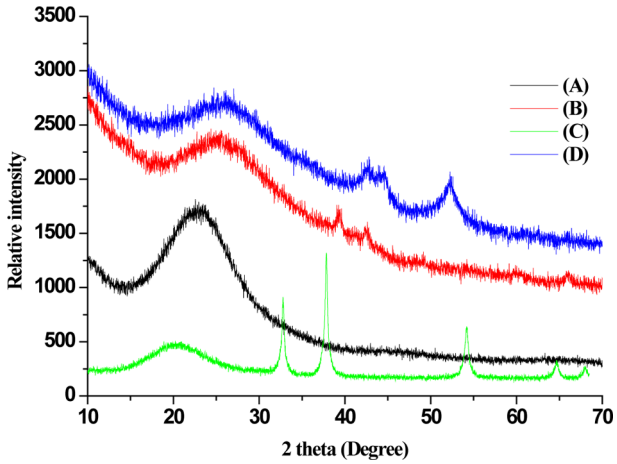

Figure 2. High angle Powder XRD of SBA-15 (A), **Fe/SBA-15** (B), **Ni/SBA-15** (C) and **Fe-Ni/SBA-15** (D).

of intensity due to phase cancellation between the pore walls and guest metal.[4-7] In high angle PXRD, the existence of major reflections corresponding to SBA-15, even after functionalization, shows that the mesoporous SBA-15 structure is retained (Figure 2). Additionally, there was a broad peak ($2\theta = 23.32°$) attributed to SiO_2 (the component of SBA-15).[5] High angle XRD peaks at $2\theta = 25.49°$, $39.35°$, $42.27°$ (**Fe/SBA-15**), $25.93°$, $32.76°$, $37.84°$, $54.19°$, $64.67°$, $67.96°$ (**Ni/SBA-15**) and $20.47°$, $42.65°$, $44.45°$, $52.25°$ (**Fe-Ni/SBA-15**) were observed for metal supported catalyst. Although the catalysts **Fe/SBA-15** and **Fe-Ni/SBA-15** contain iron metal, the catalysts are not resemble with Fe_2O_3 on mesoporous silica surface as described in high angle XRD (10-80 range). It clearly suggested that **Fe/SBA-15** and **Fe-Ni/SBA-15** retained a highly ordered structure of SBA-15 after metal incorporation. There were no obvious diffraction peaks of Fe_2O_3 on mesoporous silica in the wide angle range of the catalysts. Iron species was well dispersed over SBA-15 surface.[8] High angle PXRD pattern of the **Ni/SBA15** sample displayed the characteristic peaks corresponding to nickel oxide, too.[5,9]

Scanning Electron Microscopy (SEM) Analysis and Transmission Electron Microscopy (TEM) Analysis. SEM micrographs showed that the SBA-15 (Figure 3(a)) samples consisted of small agglomerates. The morphology was maintained after metal impregnation to form **Fe/SBA-15**, **Ni/SBA-15** and **Fe-Ni/SBA-15** (Figure 3(b), (c), (d)). The cata-

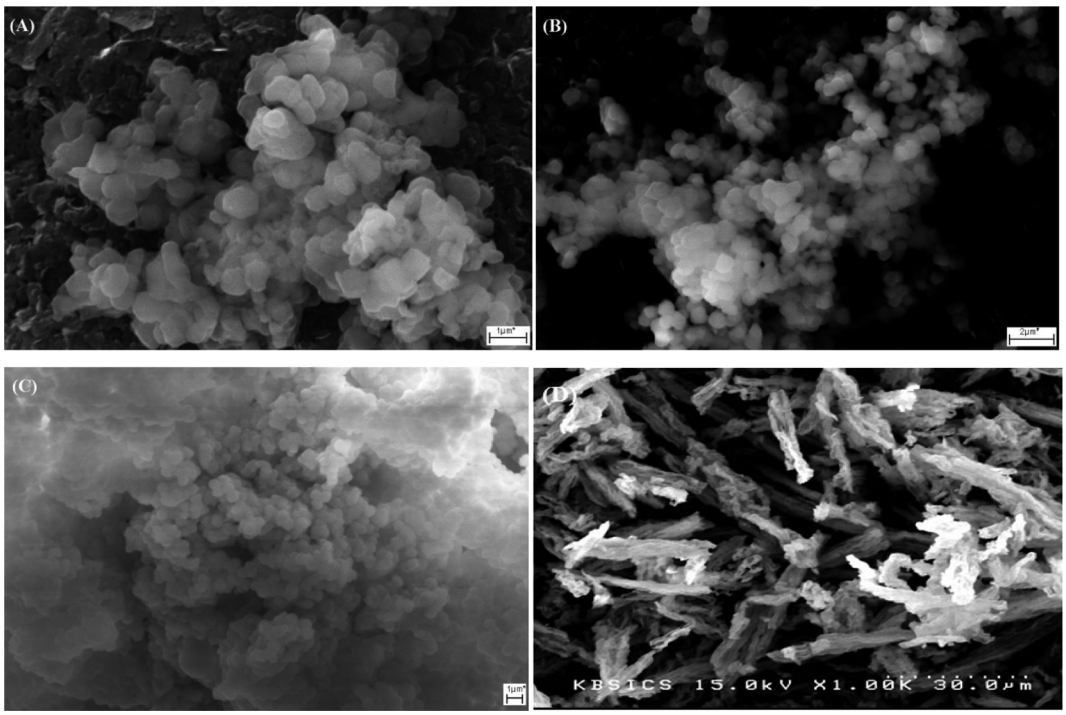

Figure 3. SEM images of SBA-15 (A), **Fe/SBA-15** (B), **Ni/SBA-15** (C) and **Fe-Ni/ SBA 15** (D).

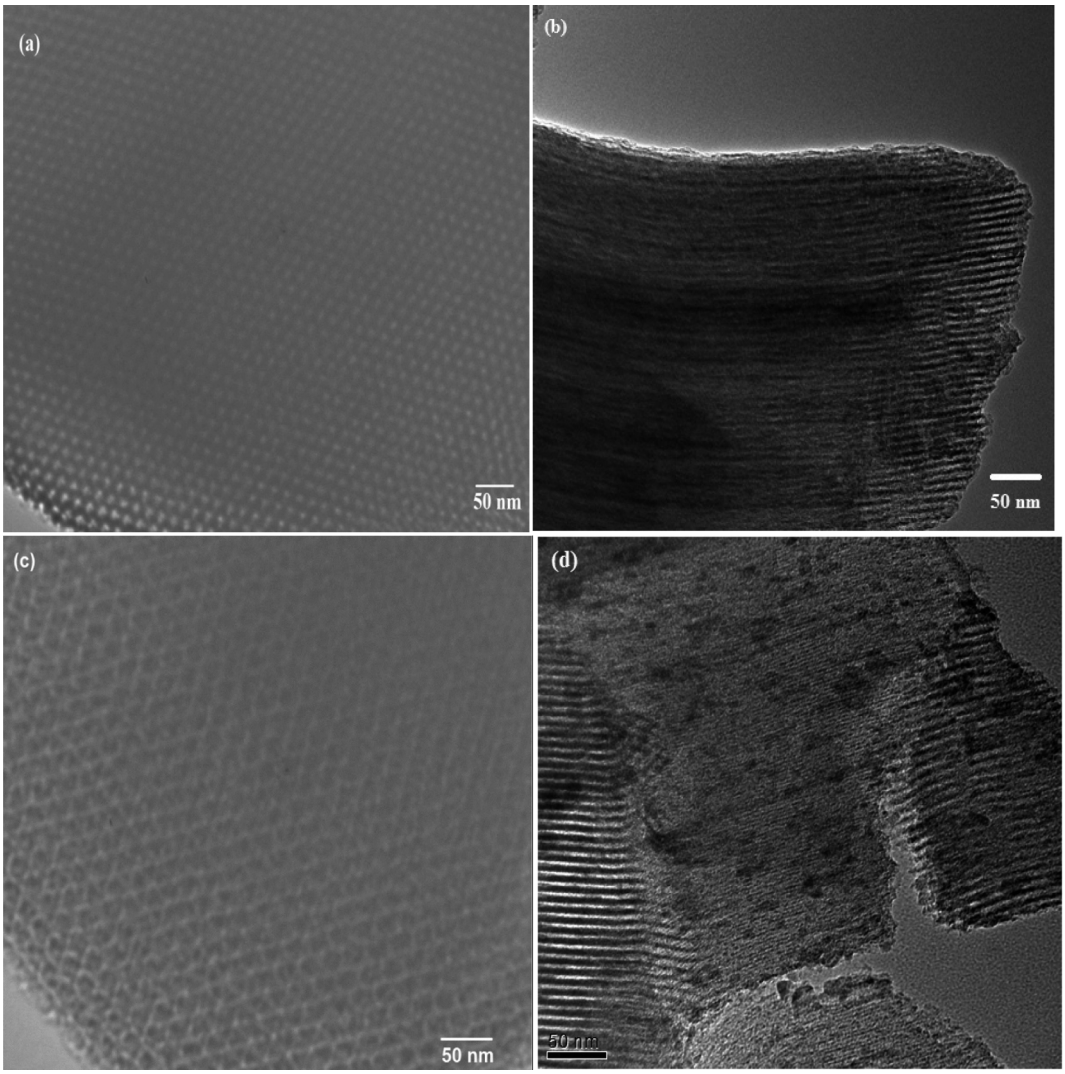

Figure 4. TEM images of SBA-15 (a), **Fe/SBA-15** (b), **Ni/SBA-15** (c) and **Fe-Ni/SBA-15** (d).

lysts revealed uniform size particles with ordered hexagonal mesoporous structure.[6,8] TEM micrographs of siliceous SBA-15 confirmed hexagonally arranged pore structures when viewed along the pore direction and parallel lattice fringes when viewed along the side (Figure 4(a)). SBA-15 synthesized in the acidic medium displayed mesopores of one-dimensional channels, indicating SBA-15 to possess a 2D p6mm hexagonal structure. The presence of equidistant parallel fringes exhibits the nature of separation between the layers and the unique well-packed arrangement of mono layers. The ordered mesoporous structure of SBA-15 was unaffected by the incorporation of the metals, as shown in **Fe/SBA-15**, **Ni/SBA-15** and **Fe-Ni/SBA-15** (Figure 4(b), (c), (d)).

Nitrogen Adsorption-desorption Isotherm Study. The N_2 adsorption–desorption isotherms of SBA-15 and as prepared catalysts **Fe/SBA-15**, **Ni/SBA-**15 and **Fe-Ni/SBA-15** showed type IV (Figure 5), which revealed the presence of ordered structure of SBA-15.[10-12] The Surface and pore characteristics data are summarized in Table 1. A large decrease in BET surface area was observed (from 795 to 512 m^2/g) upon Fe metal functionalisation on SBA-15. Similarly, a decrease in the mesoporous diameter and pore volume from 79 to 74 Å and 1.289 to 0.925 cm^3/g, respectively, was also observed (Table 1). Decreases in the BET surface area, pore diameter and pore volume from 795 to 514 m^2/g, 79 to 44 Å and 1.289 to 0.568 cm^3/g, respectively were observed upon Ni incorporation in SBA-15 (Table 1). Whereas for **Fe-Ni/SBA-15**, BET surface area, pore diameter and pore volume decreased from 795 to 728 m^2/g, 79 to 42 Å and 1.289 to 0.760 cm^3/g, respectively.

Thermogravimetric analysis. Thermo-gravimetric curves show that significant weight losses of about 3.7, 6.3, 10.1 and 14.4% occurred from 28 to 900 ^oC for **SBA-15**, **Fe/SBA-15**, **Ni/SBA-15** (Figure 6(a)) and **Fe-Ni/SBA-15** (Figure 6(b)), respectively. This weight loss can be mainly attributed to the release of water. [11] Consistent weight losses of **SBA-15**, **Fe/SBA-15**, **Ni/SBA-15** and **Fe-Ni/SBA-15** between 28 to 900 ^oC as a result of carbonization is observed.

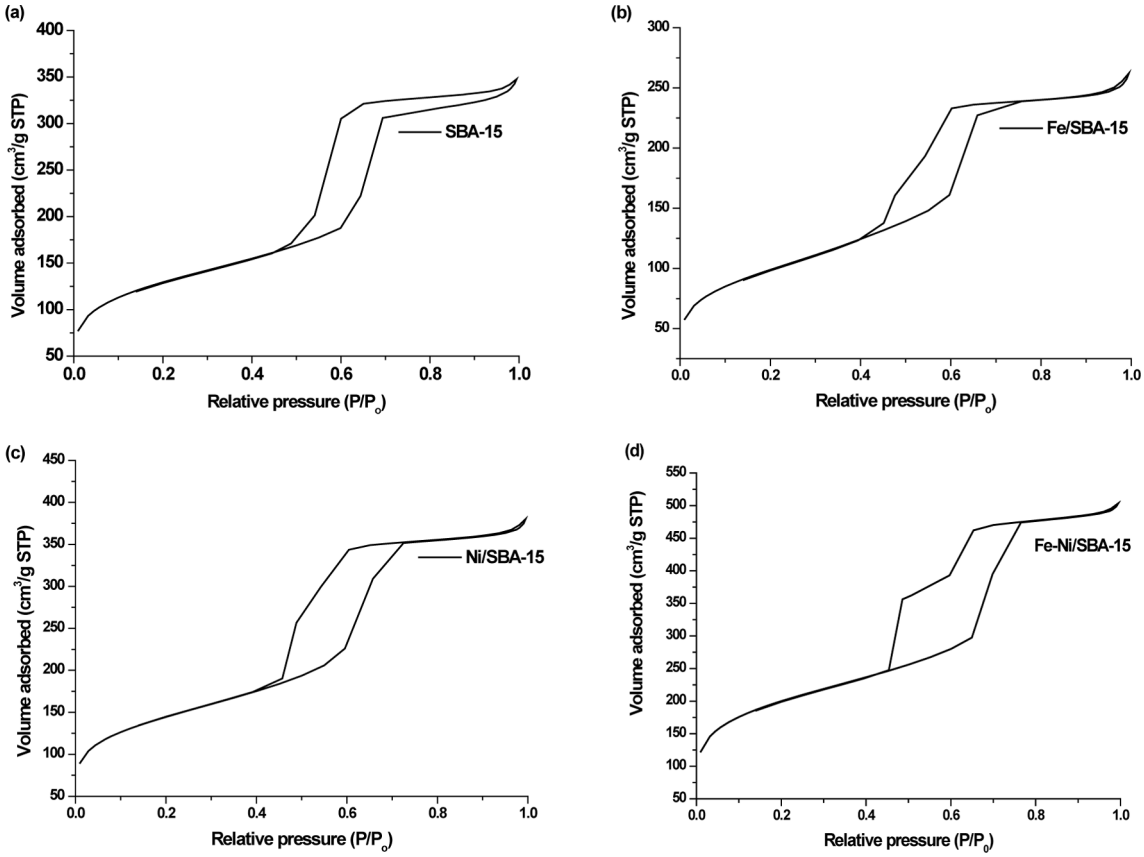

Figure 5. N_2 adsorption/desorption isotherms of **SBA-15** (a), **Fe/SBA-15** (b), **Ni/SBA-15** (c) and **Fe-Ni/SBA-15** (d).

Table 1. Surface and pore characteristics of SBA-15, **Fe/SBA-15**, **Ni/SBA-15** and **Fe-Ni/SBA-15**

Compound	BET surface area (m^2/g)	Total pore volume (cm^3/g)	BJH pore diameter (Å)
SBA-15	795	1.289	78.9
Fe/SBA-15	512	0.925	73.8
Ni/SBA-15	514	0.568	44.3
Fe-Ni/SBA-15	728	0.760	41.7

Catalytic Oxidation of Bisphenol A

Blank Experiments. Before examining the efficiency of the catalysts for the catalytic oxidation of bisphenol A, a set of blank experiments were carried out under the reaction conditions: (i) bisphenol A (5×10^{-4} mole L^{-1}) without a catalyst and H_2O_2, (ii) bisphenol A (5×10^{-4} mole L^{-1}) and H_2O_2 (1:1 molar ratio) without a catalyst, (iii) bisphenol A (5×10^{-4} mole L^{-1}) with SBA-15 as the catalyst (2 g L^{-1}), and (iv) bisphenol A (5×10^{-4} mole L^{-1}) and H_2O_2 (1:1 molar

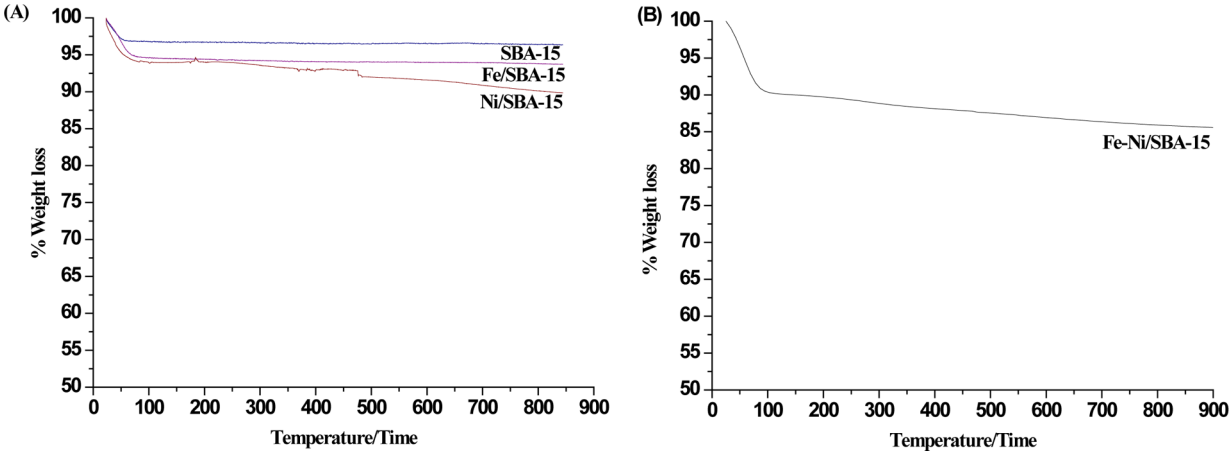

Figure 6. TGA curves of SBA-15, **Fe/SBA-15**, **Ni/SBA-15** (A) and **Fe-Ni/SBA-15** (B).

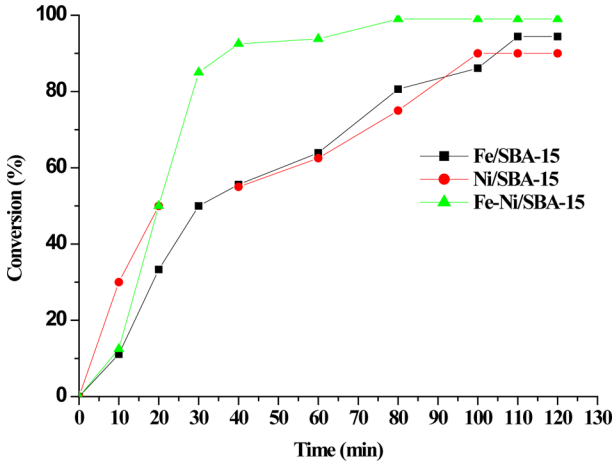

Figure 7. Effects of reaction time on catalytic oxidation of bisphenol A with **Fe/SBA-15, Ni/SBA-15** and **Fe-Ni/SBA-15** (load 2 g L^{-1}, bisphenol A: 5×10^{-4} mole L^{-1}) at 353 K.

ratio) with SBA-15 as the catalyst (2 g L^{-1}). The reactions were carried out at 298 K, atmospheric pressure, 200 rpm stirring and a time interval of 2 h. No measurable conversion could be detected for blank experiment.

Effect of the Reaction Time. An increase in the reaction time from 10 to 120 min showed enhanced bisphenol A degradation, as shown in Figure 7. In a series of reactions, which were carried out in this time interval with bisphenol A (5×10^{-4} mole L^{-1}) and H_2O_2 (5×10^{-4} mole L^{-1}) at 298 K using **Fe/SBA-15**, **Ni/SBA-15** or **Fe-Ni/SBA-15** as catalyst with a load of 2 g L^{-1}, the conversion increased from 11.1 to 94.4%, 30.0 to 90.0% and 12.5 to 99.0%, respectively. The catalysts were found to be capable catalysts, indicating that wet impregnation might have left some Fe(III), Ni(II) on the accessible sites of SBA-15, which are responsible for converting more reactants. The UV–vis measurement spectra of bisphenol A degradation by catalysts **Fe/SBA-15**, **Ni/SBA-15** or **Fe-Ni/SBA-15** is shown in Figure 8. The absorbance peak became weaker in intensity with time and totally disappeared after 110 min, 100 min and 80 min with the catalysts **Fe/SBA-15**, **Ni/SBA-15** and **Fe-Ni/SBA-15**, respectively. This indicates that the bisphenol A was degraded totally into its mineral components. Similar results were reported by Fenton and sono-Fenton bisphenol A degradation by Ioan *et al*. (2007),[13] but they did not report the final products of the reaction. In our work, the products of the catalytic degradation of bisphenol A were monitored by GC-MS analysis also (Scheme 1).

Effect of pH for Leaching Experiment. As the catalysts **Fe/SBA-15**, **Ni/SBA-15** and **Fe-Ni/SBA-15** contain transition metal ions (Fe^{3+}, Ni^{2+}), it is important to see whether they cause secondary pollution after use. The leaching of the metals from the catalysts was studied by vigorously agitating 0.1 g of the catalysts with 50 mL water at pH 3.0, 4.0, 5.0, 6.0, 7.0, 8.0, and 9.0 at 298 K (the temperature at which the wet oxidation reactions were carried out) for 2 h. The mixture was centrifuged and the amounts of Fe and Ni in the

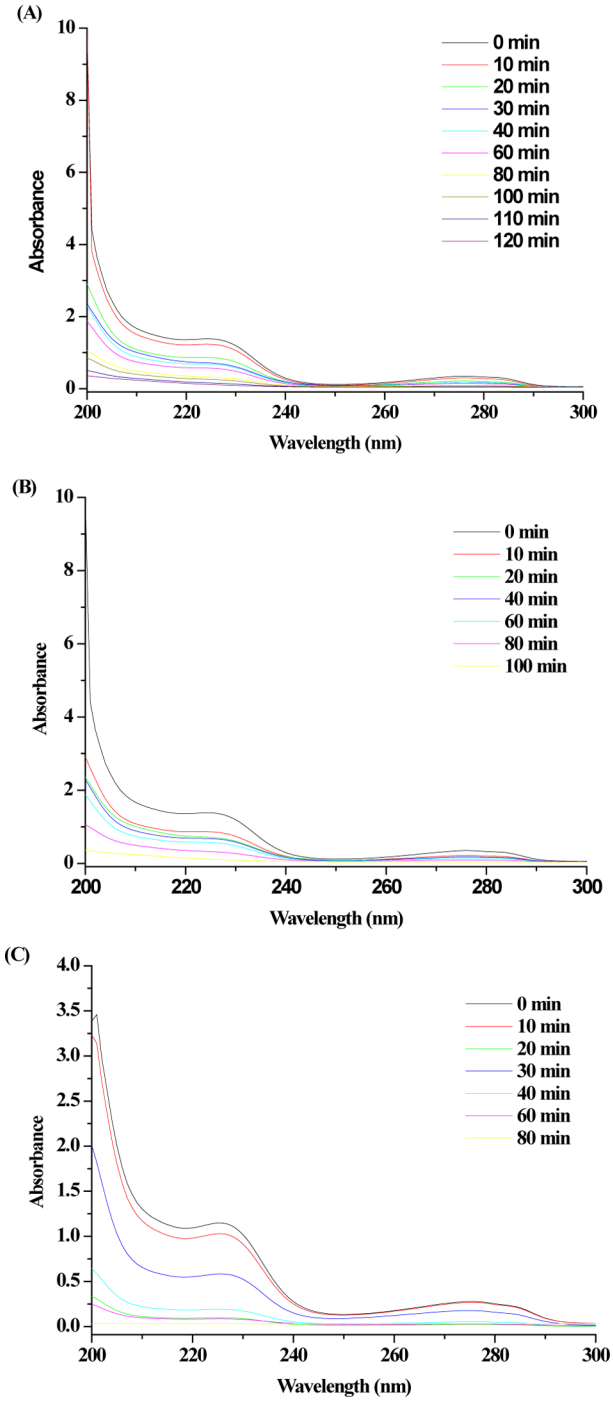

Figure 8. Time dependant UV-vis spectra of bisphenol A solutions with **Fe/SBA-15** (A), **Ni/SBA-15** (B) and **Fe-Ni/SBA-15** (C). Reaction conditions: bisphenol A 5×10^{-4} mole L^{-1}, load 2 g L^{-1}, temperature 353 K.

aqueous layer were determined. Fe released by **Fe/SBA-15** was between 0.50 and 1.18%, Ni released by **Ni/SBA-15** was from 0.03 and 0.14% and from **Fe-Ni/SBA-15** catalyst 0.25 to 0.99% (Fe) and 0.01 to 0.12% (Ni), respectively.

The pH of the medium has significant influence on the leaching, but it was found that maximum release occurred at basic medium. The leaching in general is very small and does not give rise to concentration of the metals in water,

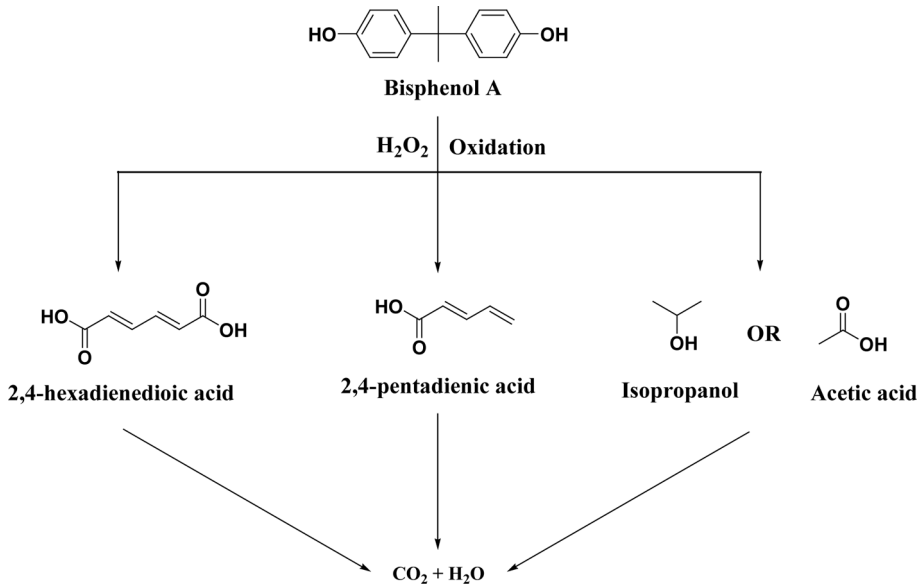

Scheme 1. Main degradation pathways of bisphenol A during wet catalytic oxidation.

which are higher than the permissible values even when drinking water quality is considered. The leachability experiment has shown that the amount of Fe and Ni released into water will give rise to a concentration of Fe and Ni far below the World Health Organization guideline[14] value (for Fe(III) in natural fresh water ranges from 0.5 to 50 mg L^{-1} and for Ni in drinking water 0.02 mg L^{-1}). Thus, the use of the catalysts is not likely to create problem of water contamination.

Effect of Temperature. Although most of the experiments in this work were done at 298 K (close to room temperature), separate sets of experiments were designed to look into the effect of increasing temperature on bisphenol A degradation. Very small increase in the degradation was observed (Table 2) as the reaction was run successively at 288, 298, 303, 308 and 313 K. The increase in the degradation efficiency of the catalysts are evidently due to increased mobility of the bisphenol A molecules at higher temperature as well as their improved diffusional transport from the bulk phase to the liquid-catalyst interface. The oxidative degradation of bisphenol A with the catalysts, **Fe/SBA15**, **Ni/SBA15** and **Fe-Ni/SBA-15** were enhanced from 94.0-95.0%, 89.6-90.7% and 98.1-99.4%, respectively as the reaction was carried out at 288 K and 313 K. Similar trends were observed by Tang *et al.* (2011)[15] in catalytic removal of bisphenol A from aqueous solution with hemoglobin immobilized on amino modified magnetic nano particles as an enzyme catalyst.

Table 2. Effects of reaction temperature on catalytic oxidation of bisphenol A with **Fe/SBA-15, Ni/SBA-15** and **Fe-Ni/SBA-15** (load 2 g L^{-1}, bisphenol A: 5×10^{-4} mole L^{-1})

Temperature (K)	Conversion (%)		
	Fe/SBA-15	Ni/SBA-15	Fe-Ni/SBA-15
288	94.0	89.6	98.1
298	94.4	90.0	99.0
303	94.5	90.2	99.2
308	94.8	90.4	99.4
313	95.0	90.7	99.4

Product Analysis

The identification of reaction products from the wet catalytic oxidation of BPA was carried out with metal impregnated SBA-15 catalysts by means of the GC-MS analytical method (Scheme 1). The mechanism is based on •OH radicals. These radicals have their origin either in metal oxides formed during calcination of the catalysts or in the breaking of hydrogen peroxide (or water) molecules under the influence of the transition metal cations. The formation of •OH radicals on the surface of the catalysts will follow from interactions between the excited O-atoms of the catalyst and H-atoms cleaved from the substrate or even water because the reactions were carried out in an aqueous solution. The participation of dissolved oxygen in •OH radical

Table 3. Main bisphenol A intermediates identified by GC-MS

Peak No.	*m/z*	Molecular weight	Molecular structure	Product names
1	59	60	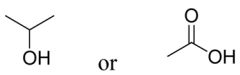	Isopropanol or acetic acid
2	97	98	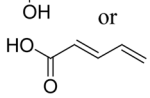	2,4-pentadienic acid
3	141	142	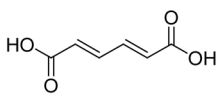	2,4-hexadienedioic acid
4	227	228	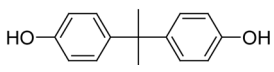	Bisphenol A

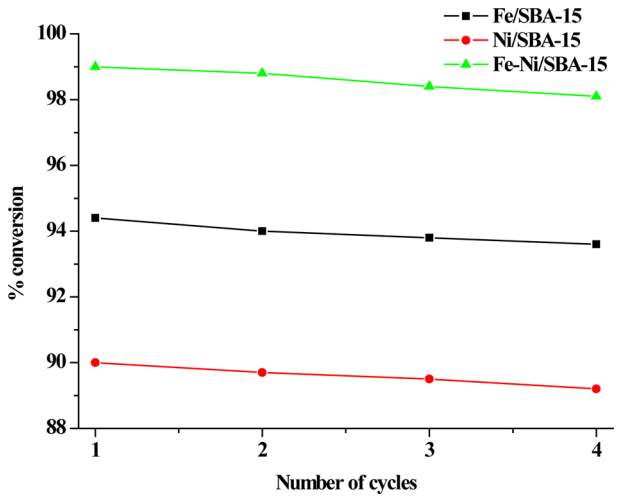

Figure 9. Efficiency of the catalysts, **Fe/SBA-15**, **Ni/SBA-15** and **Fe-Ni/SBA-15** in four consecutive cycles of bisphenol A oxidation.

formation is unlikely because this will result in a drastic reduction in oxidation with increasing reaction temperature (consequent to a decrease in dissolved oxygen level).[16] GC-MS analysis identified the following: 2,4-hexadienedioic acid, 2,4-pentadienic acid and isopropanol or acetic acid (Table 3). Subsequent oxidation of these intermediate products led to CO_2 and H_2O.[15]

Recyclability of the Catalysts

An attempt was made to recycle the catalysts **Fe/SBA-15**, **Ni/SBA-15** or **Fe-Ni/SBA-15** after catalytic oxidation of bisphenol A under the optimized reaction conditions. After the first catalytic reaction in the presence of H_2O_2, the catalyst was isolated by filtration and the solid mass was Soxhlet-extracted with ethanol and water. The recovered solid was then dried in a vacuum desiccator overnight and used directly as catalyst in the next catalytic reaction. Four catalytic runs were carried out successfully with the same catalyst with no observable loss in performance (Figure 9).

References

1. Zhao, D.; Huo, Q.; Feng, J.; Chmelka, B. F.; Stucky, G. D. *J. Am. Chem. Soc.* **1998**, *120*, 6024-6036.
2. Zhao, D.; Feng, J.; Huo, Q.; Melosh, N.; Fredrickson, G. H.; Chmelka, B. F.; Stucky, G. D. *Science* **1998**, *279*, 548-552.
3. Vinu, A.; Sawant, D. P.; Ariga, K.; Hossain, K. Z.; Halligudi, S. B.; Hartmann, M.; Nomura, M. *Chem. Mater.* **2005**, *17*, 5339-5345.
4. Mayani, S. V.; Mayani, V. J.; Kim, S. W. *Canad. J. Chem. Eng.* **2013**, *91*(7), 1270-1280.
5. Liu, H.; Li, Y.; Wu, H.; Takayama, H.; Miyake, T.; He, D. *Catal Comm.* **2012**, *28*, 168-173.
6. Shukla, P.; Wang, S.; Sun, H.; Ang, H.-M.; Tade, M. *Chem. Eng. J.* **2010**, *164*, 255-260.
7. Brieler, F. J.; Grundmann, P.; Froba, M.; Chen, L.; Klar, P. J.; Heimbrodt, W.; Nidda, H. A. K. V.; Kurz, T.; Loidl, A. *J. Am. Chem. Soc.* **2004**, *126*, 797-807.
8. Huang, R.; Yan, H.; Li, L.; Deng, D.; Shu, Y.; Zhang, Q. *Appl. Catal. B: Environ.* **2011**, *106*, 264-271.
9. Jung, H.; Kim, J.-W.; Cho, Y.-G.; Jung, J.-S.; Lee, S.-H.; Choi, J.-G. *Appl. Catal. A: General* **2009**, *368*, 50-55.
10. Chiang, H.-L.; Wu, T.-N.; Ho, Y.-S.; Zeng, L.-X. *J. Hazard. Mater.* **2014**, *276*, 43-51.
11. Calles, J. A.; Carrero, A.; Vizcaino, A. J. *Microporous Mesoporous Mater.* **2009**, *119*, 200-207.
12. Zhao, M.; Church, T. L.; Harris, A. T. *Appl. Catal. B: Environ.* **2011**, *101*, 522-530.
13. Ioan, I.; Wilson, S.; Lundanes, E., Neculai, A. *J. Hazard. Mater.* **2007**, *142*, 559-563.
14. WHO, Guidelines for Drinking-Water Quality, (2004) 3rd edn. 1: Recommendations, (World Health Organization, Geneva.
15. Tang, T.; Fan, H., Ai, S.; Han, R.; Qiu, Y. *Chemosphere* **2011**, *83*, 255-264.
16. Stoyanova, M.; Christoskova, St.; Georgieva, M. *Appl. Catal. A: General* **2003**, *249*, 295-302.